Published in Contributions to Mineralogy and Petrology 147, issue 3, 330-345, 2004,
which should be used for any reference to this work

B. Kober · A. Kalt · M. Hanel · R. T. Pidgeon

SHRIMP dating of zircons from high-grade metasediments of the Schwarzwald/SW-Germany and implications for the evolution of the Moldanubian basement

Abstract Four metasedimentary zircon populations from different tectonometamorphic units of the Central and the Northern Schwarzwald (Variscan belt, SW-Germany) were investigated using SEM, cathodoluminescence and SHRIMP dating. Despite partially strong modifications of primary internal morphologies during Variscan metamorphism at amphibolite (750 °C, 0.4–0.6 GPa) and granulite-facies conditions (950–1,000 °C, 1.4–1.8 GPa), many grains show well-preserved protolith ages. The detritus indicates a northern Gondwana origin and different **Palaeozoic** episodes of sediment deposition and consolidation. Two of the studied sediments were deposited in Cambrian/early-Ordovician times and consolidated in positions close to northern Gondwana. Late Ordovician and rare Devonian detritus from sediments of two other tectonometamorphic units indicates much later sedimentation close to the leading edge of Gondwana or a terrane assemblage during northern drift towards Laurussia. Subsolidus growth of new zircon due to Variscan granulite facies metamorphism of one of the tectonometamorphic units is precisely dated at 335 ± 2 Ma.

B. Kober (✉)
Institut für Umwelt-Geochemie,
Ruprecht-Karls-Universität,
Im Neuenheimer Feld 236,
69120 Heidelberg, Germany
E-mail: bernd.kober@urz.uni-heidelberg.de

A. Kalt
Institut de Géologie, Université de Neuchâtel,
Rue Emile Argand 11 / CP 2,
2007 Neuchâtel, Switzerland

M. Hanel
Mineralogisches Institut,
Ruprecht-Karls-Universität,
Im Neuenheimer Feld 236,
69120 Heidelberg, Germany

R. T. Pidgeon
Curtin University of Technology, GPO Box U1987,
6845 Perth, WA, Australia

Introduction

Single zircon dating is a powerful tool for investigating sediment provenances and estimating sedimentation ages (e.g. Aleinikoff et al. 1988; Lork et al. 1990; Robb et al. 1990; Davis et al. 1990; Ross et al. 1991; McLennan et al. 2001). Where sedimentary sources have suitable lithological characteristics it is possible to constrain the duration of sedimentation episode(s) by evaluating the detrital zircon age distribution (e.g. Nelson 2001). Detritus ages and times of sediment deposition are important for discussions of sediment sources and continental drift models (e.g. Gebauer et al. 1989; Nance and Murphy 1996; Friedl et al. 2000). Sediment provenance and sedimentation ages are crucial to unravelling the orogenic and pre-orogenic history of mountain belts. In the Variscan fold belt detritus ages have been successfully used to detect ancient terranes and to reconstruct the geodynamic and geotectonic evolution of Europe during the Palaeozoic (e.g. Franke 2000; Hegner and Kröner 2000; Linnemann et al. 2000; Söllner et al. 1997; Tichomirova et al. 2001; von Raumer et al. 2002, 2003). The contribution of detrital zircon dating is most important in the understanding of the internal parts of orogens where complex internal nappe structures and high-grade metamorphism often impede the application of palaeomagnetic, stratigraphic and palaeontological methods. In the Variscan belt, however, there are only few studies of detrital components from high-grade metasediments (e.g. Zeh et al. 2001). The present work focuses on detrital zircon ages from high-grade metamorphic sediments of the Schwarzwald as part of the internal Variscan belt. We will show that even zircons from granulite-facies metasediments can serve to characterize sediment provenance and to constrain the premetamorphic evolution of these rocks.

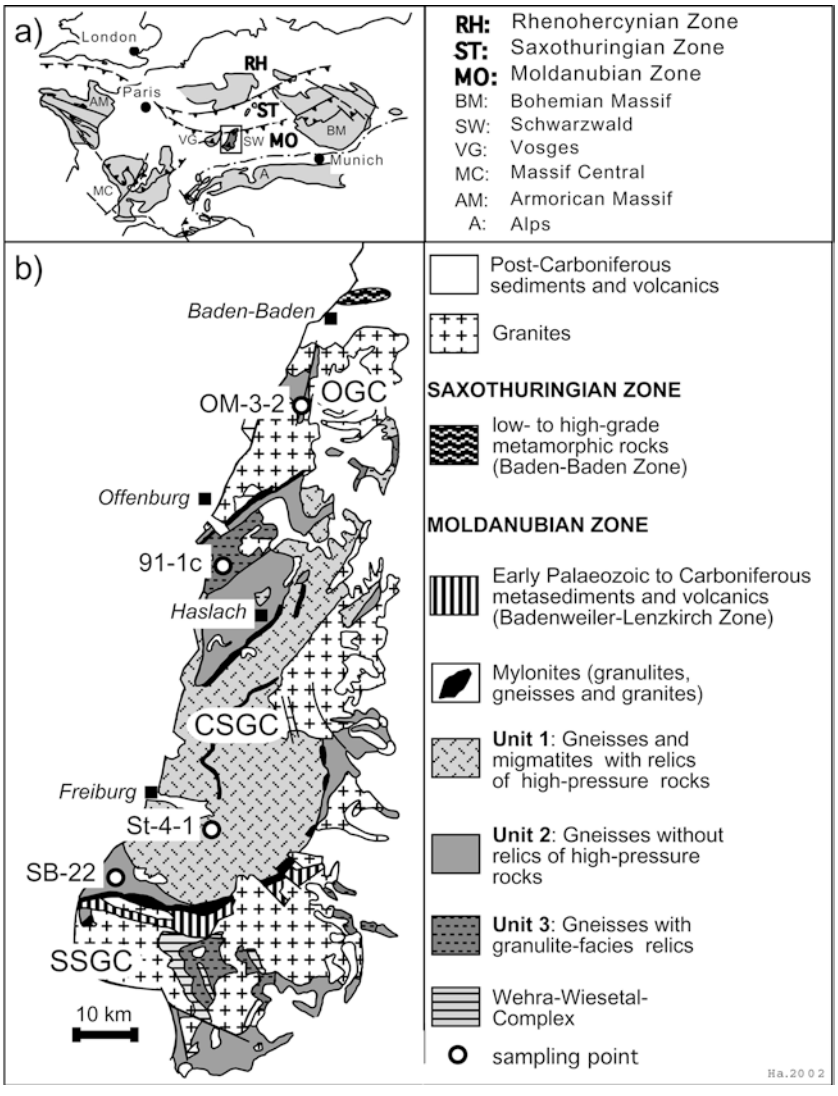

Fig. 1 Sketch map showing **a** the position of the Schwarzwald and other units in the crystalline basement rocks of Central Europe; **b** the Central Schwarzwald Gneiss Complex (CSGC) and the northern Schwarzwald (Omerskopf, OGC), tectonometamorphic units of the Central Schwarzwald basement, and sample locations. (*SSGC* Southern Schwarzwald Gneiss Complex)

Geodynamic and palaeogeographic context

The Variscan fold belt can be traced from the Appalachian and Ouitchita Mountains in the west via Europe to the Caucasus in the east. It formed by Devonian to Carboniferous accretion and collision processes between Laurussia in the north, Gondwana in the south and different terranes and microcontinents in between. The latter are generally seen as derived from the northern margin of Gondwana (e.g. Franke 2000; von Raumer et al. 2002) during Palaeozoic rifting events. From the Neoproterozoic to the Ordovician, they are viewed as an EW-trending belt comprising from west to east Avalonia, the Amorican terrane assemblage (ATA) and the Cadomian terranes, the future Alpine realm, and parts of future Asia (e.g. Scotese and McKerrow 1990, Tait et al. 1994, 1995; Stampfli et al. 2002, von Raumer et al. 2002, 2003). In the Silurian, Avalonia had already collided with the northern continents, whereas the other parts of the belt remained close to Gondwana. The subsequent motion of the microplates and opening or closure of ocean basins has been modelled by alternative concepts (e.g. Scotese and McKerrow 1990; Tait et al. 2000; Matte 2001; Cocks and Torsvik 2002; Stampfli and Borel 2002). For a critical discussion e.g. of the Armorica microplate concept we refer to Robardet (2003) and references therein.

In central Europe, the isolated Variscan basement outcrops found today have been divided into several EW-trending zones according to their grade of metamorphism and their magmatic intrusions (Kossmat 1927). Within this scheme, the southern margin of the Northern Phyllite Zone is thought to represent the Rheic suture, separating the Avalonia-derived Rhenohercynian Zone in the north from the Armorica- or Hun-derived Mid-German Crystalline High and the Saxothuringian and Moldanubian zones in the south (Fig. 1). However, due to large-scale lateral transfer and escape along the Eurasian margin in Carboniferous times (Stampfli et al. 2002) these zones do not necessarily correspond to ancient terrane boundaries. Also, the pre-Variscan provenance of the predominantly high-grade

Saxothuringian and Moldanubian zones is only poorly understood. Within this context, the Schwarzwald and the Vosges in the southwestern part of the Moldanubian zone are of particular interest. Geographically, they are located between the Armorican Massif, classically considered to represent the terrane Armorica, and the Moldanubian zone of the Bohemian Massif, seen as a more easterly part of the European Hunic *terrane* by several authors (Stampfli et al. 2002; von Raumer et al. 2002). Lithologically, apart from granites, the Schwarzwald and Vosges are dominated by high-grade metamorphic gneisses and migmatites.

Geological setting and samples

The samples for this study were taken from the Central Schwarzwald Gneiss Complex (CSGC) and the Omerskopf Gneiss Complex (OGC). Both complexes belong to the southwestern part of the Moldanubian zone (e.g. Franke 2000, Fig. 1). On the basis of metamorphic grade, lithology and high-grade metamorphic relics the CSGC was divided into three different tectonometamorphic units (Hanel and Wimmenauer 1990; Hanel et al. 1999; Fig. 1). Unit 1 of the CSGC is dominated by paragneisses and migmatites with relics of eclogite-facies and mantle-derived rocks. Unit 2 consists of more variegated gneisses and is devoid of high-pressure relics, but with rare evidence for an older medium-pressure medium-temperature stage (Rehfeld 1983). Unit 3 is characterized by granulite-facies relics and rare eclogites and mantle-derived rocks, and is mainly found in the northern part of the CSGC (Fig. 1, Hanel et al. 1993). Peak equilibration conditions of the granulites were approximately 950–1,000 °C and 1.4–1.8 GPa, and the entire unit is interpreted as part of the lower crust of a hanging continental plate in a convergent Variscan setting (Marschall et al. 2003). While Unit 1 is in the tectonically uppermost position, there is some evidence that Unit 3 overlies Unit 2 (Kalt et al. 2000). All three units were subjected to a final high-temperature low-pressure metamorphic event at about 330 Ma (Kalt et al. 1994; Lippolt et al. 1994), with P–T conditions of 730–780 °C and 0.42–0.45 GPa (Kalt et al. 2000). The pre-metamorphic history and the depositional conditions of the metasediments in the Schwarzwald are very roughly constrained by palynological data (Montenari 1996; Hann and Sawatzki 1998; Hanel et al. 1999; Montenari et al. 2000), which are consistent with sediment deposition in Neoproterozoic to Early Palaeozoic marine environments. The genetic relations between the metasediments hosted in the tectonometamorphic units, the timing of sediment deposition, and the palaeogeographic positions of the corresponding marine basins are yet unknown.

For this study, three paragneiss samples were selected to represent the tectonometamorphic Units 1–3 (Fig. 1): St-4-1 (Unit 1), SB-22 (Unit 2), 91-1c (Unit 3). A fourth sample (OM-3-2, Fig. 1) was taken from the OGC. The relation of the OGC to the CSGC units is unclear because it is separated from the main part of the CSGC by Carboniferous granites and shear zones. While sample 91-1c is a pelitic garnet-cordierite-sillimanite gneiss, the other investigated rocks are plagioclase-biotite-quartz gneisses, probably derived from greywackes (Müller 1989).

Analytical procedures

Zircon grain size fractions were separated from 2–4 kg of each of the rock samples following routine preparation procedures. Several hundred zircon grains from the 100–200 μm size fraction were embedded in epoxy resin for a comprehensive SEM and cathodoluminescence (CL) documentation of the internal grain morphologies. This documentation was a prerequisite for the recognition of zircon subpopulations in the investigated rocks, for the preselection of grains representative of the distribution of zircon phases in the different zircon populations, and for the choice of suitable spot locations on the polished internal surfaces of the grains selected for ion probe analysis (SHRIMP, Compston et al. 1984). The procedures applied for the U-Th-Pb isotope analyses using the SHRIMP II instrument at Curtin University/Perth-Australia are described in detail e.g. by Nemchin and Pidgeon (1997) and by De Laeter and Kennedy (1998). Fragments of the gem Sri Lankan zircon CZ3 were embedded in the mounts together with the sample zircons and used as a standard reference (Pidgeon et al. 1994). A $^{206}Pb/^{238}U$ value of 0.0914 corresponding to an age of 564 Ma was used for the calculation of ages. Data were reduced using the Perth in-house programs (Kinny, personal communication) and the ISOPLOT program of Ludwig (2000). Broken Hill Pb isotope composition was assumed for the common Pb correction, according to the composition of the applied gold coating of the mounts.

Reproducibility of the normalizing standard U/Pb ratio ranged between 1.5 and 2.3% for the different data sets. Errors given in Table 1 and in the data plots (Fig. 2) are overall errors on the one sigma standard deviation level, including counting statistics, ^{204}Pb-correction and the U/Pb ratio reproducibility calculated from the repeated U/Pb measurements of the standard fragments.

Results

SHRIMP results are presented in Table 1 and on concordia plots in Fig. 2. CL images of representative grains with SHRIMP analytical spots are shown on Fig. 3.

Morphological comparisons

It can be seen that the investigated zircon populations are complex, with subpopulations consisting of euhedral grains with characteristic oscillatory or sector zoning, and rounded or irregularly shaped grains with irregular or patchwork-like internal zoning. Many grains show core/rim associations, and/or have patchy zones with enhanced luminescence. The preservation of euhedral crystal shapes in the sedimentary subpopulations is striking. A common feature of all the investigated populations is frequent partial modification and obliteration of igneous oscillatory zoning, and the generation of secondary internal structures, showing transgressive recrystallization with recrystallization fronts and

Table 1 U-Pb SHRIMP data of four metasedimentary zircon populations from the Schwarzwald. Isotope ratios are corrected for common Pb using the ^{204}Pb-concentration. *%conc* %concordance = 100x (age ^{206}Pb/^{238}U)/(age ^{207}Pb/^{206}Pb). Errors are at the 1 sigma standard deviation level. *c* core; *r* rim; *oz* oscillatory zoning; *sz* sector zoning; *wl* weak luminescence; *wil* weak irregular luminescence; *sl* strong luminescence; *sp* short prismatic; *lp* long prismatic; *ro* rounded

Spot	Comment	U/ppm	Th/ppm	Th/U	Pb/ppm	207/206-4	+/-	208/206-4	+/-	207/235-4	+/-	206/238-4	+/-	% conc	Age 206/238	+/-	Age 207/235	+/-	Age 207/206	+/-
Sample St-4-1. "unit 1"																				
st41-6-1a	oc,oz,sp	72	20	0.274	7	0.0525	0.0068	0.0596	0.0164	0.6158	0.0822	0.0851	0.0018	172	527	11	487	52	306	270
st41-6-1b	oc,oz,sp	99	30	0.306	9	0.0577	0.0011	0.0969	0.0021	0.7336	0.0217	0.0923	0.0019	110	569	11	559	13	517	42
st41-6-1c	r,oz	77	23	0.298	7	0.0549	0.0063	0.0789	0.0151	0.6846	0.0818	0.0904	0.0020	137	558	12	530	49	408	259
st41-14-1a	oz,lp	182	104	0.572	19	0.0603	0.0014	0.1847	0.0036	0.8007	0.0257	0.0962	0.0018	96	592	11	597	14	616	51
st41-16-1a	wl,ro	2,526	908	0.359	185	0.0548	0.0004	0.1604	0.0021	0.5217	0.0107	0.0691	0.0012	107	431	7	426	7	403	18
st41-16-1b	wl,ro	2,197	444	0.202	145	0.0530	0.0008	0.0583	0.0023	0.4736	0.0121	0.0649	0.0012	124	405	7	394	8	327	36
st41-16-2a	c,sz,sp	174	62	0.359	16	0.0579	0.0013	0.1093	0.0030	0.7185	0.0217	0.0900	0.0017	106	555	10	550	13	526	48
st41-16-3a	c,oz,sp	377	155	0.409	36	0.0597	0.0008	0.1268	0.0019	0.7766	0.0183	0.0943	0.0017	98	581	10	584	10	593	28
st41-17-1a	wl,lp	952	1,446	1.518	117	0.0590	0.0004	0.4621	0.0017	0.7606	0.0151	0.0935	0.0017	101	576	10	574	9	568	15
st41-18-1a	c,sl,sz	156	88	0.563	16	0.0593	0.0016	0.1761	0.0040	0.7798	0.0271	0.0954	0.0018	102	588	11	585	15	577	58
st41-18-1b	r,sl,oz	99	34	0.342	10	0.0623	0.0026	0.1138	0.0060	0.8221	0.0392	0.0957	0.0019	86	589	11	609	22	685	88
st41-18-2a	wl	351	187	0.534	36	0.0601	0.0010	0.1681	0.0026	0.7941	0.0210	0.0958	0.0017	97	590	10	594	12	607	37
st41-18-2b	il	300	143	0.477	31	0.0591	0.0010	0.1444	0.0026	0.7995	0.0213	0.0981	0.0018	106	603	10	597	12	571	38
st41-18-2c	il,sp	152	53	0.349	15	0.0567	0.0021	0.0963	0.0051	0.7665	0.0340	0.0980	0.0018	125	602	11	578	20	482	84
st41-19-1a	oz,wl,sp	1,508	2,379	1.577	169	0.0576	0.0003	0.5065	0.0016	0.6583	0.0127	0.0829	0.0015	100	514	9	514	8	514	13
st41-19-1b	oz,wl,sp	1,023	545	0.533	101	0.0589	0.0004	0.1626	0.0011	0.7636	0.0151	0.0940	0.0017	103	579	10	576	9	564	15
st41-19-2a	oz,lp	288	129	0.448	28	0.0589	0.0012	0.1370	0.0030	0.7665	0.0227	0.0943	0.0017	103	581	10	578	13	564	46
st41-19-2b	oz,lp	372	141	0.378	36	0.0583	0.0008	0.1140	0.0020	0.7677	0.0189	0.0955	0.0017	109	588	10	578	11	541	32
st41-19-3a	c,wil,sp	383	60	0.158	33	0.0612	0.0009	0.0495	0.0019	0.7625	0.0189	0.0904	0.0017	86	558	10	575	11	646	30
st41-19-4a	will,lp	552	173	0.313	53	0.0595	0.0006	0.0965	0.0013	0.7965	0.0170	0.0971	0.0017	102	597	10	595	10	585	21
st41-20-1a	oz,lp	227	110	0.483	23	0.0604	0.0020	0.1468	0.0049	0.7770	0.0312	0.0933	0.0018	93	575	10	584	18	617	72
st41-20-1b	oz,lp	239	109	0.458	27	0.0555	0.0042	0.1426	0.0101	0.6685	0.0533	0.0873	0.0017	125	540	10	520	32	433	168
st41-20-1c	oz,lp	226	107	0.474	23	0.0577	0.0020	0.1351	0.0048	0.7675	0.0315	0.0965	0.0018	115	594	11	578	18	517	75
st41-20-2a	c,il	227	63	0.277	22	0.0599	0.0014	0.0834	0.0034	0.8085	0.0259	0.0979	0.0018	100	602	11	602	15	601	52
st41-20-2b	oc,oz	928	115	0.124	84	0.0594	0.0004	0.0363	0.0009	0.7882	0.0159	0.0963	0.0017	102	592	10	590	9	581	16
st41-20-2c	r,oz,sp	189	136	0.721	21	0.0552	0.0019	0.2108	0.0049	0.7401	0.0307	0.0972	0.0018	142	598	11	562	18	422	78
st41-20-3a	wl	472	269	0.570	48	0.0590	0.0009	0.1793	0.0023	0.7604	0.0189	0.0935	0.0017	102	576	10	574	11	566	32
st41-20-3b	oz,sp	439	152	0.346	42	0.0606	0.0007	0.1067	0.0015	0.7985	0.0177	0.0955	0.0017	94	588	10	596	10	626	23
st41-22-1a	oz,lp	784	193	0.247	71	0.0577	0.0008	0.0721	0.0017	0.7319	0.0187	0.0919	0.0018	109	567	11	558	11	520	31
st41-22-1b	oz,lp	523	65	0.124	46	0.0567	0.0009	0.0344	0.0021	0.7132	0.0185	0.0913	0.0016	118	563	10	547	11	478	37
st41-22-2a	c,sz,sl	55	120	2.190	8	0.0584	0.0039	0.6639	0.0129	0.7489	0.0552	0.0931	0.0020	105	574	12	568	32	544	148
st41-22-2b	r,oz	1,967	94	0.048	151	0.0566	0.0007	0.0117	0.0016	0.6173	0.0141	0.0790	0.0014	103	490	8	488	9	478	27
st41-22-2c	r,oz,sp	706	42	0.060	62	0.0583	0.0006	0.0175	0.0012	0.7630	0.0168	0.0949	0.0017	108	585	10	576	10	541	23
st41-23-1a	c,oz	358	194	0.541	108	0.1170	0.0005	0.1672	0.0010	4.3859	0.0830	0.2720	0.0049	81	1,551	25	1,710	16	1910	7
st41-23-1b	r,wl,ro	1,288	47	0.037	127	0.0616	0.0005	0.0099	0.0009	0.9018	0.0182	0.1062	0.0019	99	651	11	653	10	659	16
st41-24-1a	oz,lp	521	211	0.405	48	0.0575	0.0009	0.1218	0.0021	0.7186	0.0180	0.0906	0.0016	109	559	10	550	11	512	33
st41-24-1b	oz,lp	312	61	0.196	27	0.0560	0.0015	0.0507	0.0035	0.6880	0.0234	0.0891	0.0016	122	550	10	532	14	452	59
st41-25-1a	wl	387	286	0.738	42	0.0594	0.0008	0.2239	0.0022	0.7969	0.0190	0.0974	0.0018	103	599	10	595	11	580	29
st41-25-2a	r,wl,sp	2,014	782	0.388	206	0.0601	0.0004	0.1142	0.0010	0.8262	0.0163	0.0996	0.0018	101	612	10	611	9	608	15
st41-25-2b	c,il	483	361	0.748	64	0.0589	0.0023	0.2177	0.0059	0.8626	0.0398	0.1062	0.0020	115	651	12	632	22	564	86
st41-25-3a	sz,sp	199	63	0.315	21	0.0610	0.0007	0.0948	0.0015	0.8909	0.0203	0.1060	0.0020	102	649	12	647	11	638	24
Sample OM-3-2. OGC																				
om32-12-1a	oz,sp	630	285	0.452	62	0.0581	0.0008	0.1342	0.0019	0.7618	0.0200	0.0951	0.0020	110	586	12	575	12	533	29
om32-12-2a	oz,sp	437	136	0.311	40	0.0596	0.0007	0.0988	0.0017	0.7498	0.0192	0.0912	0.0019	95	563	11	568	11	590	27
om32-14-1a	oz,sp	465	329	0.708	48	0.0587	0.0007	0.2291	0.0020	0.7481	0.0191	0.0924	0.0019	102	570	11	567	11	557	27

Table 1 (contd.)

Spot	Comment	U/ppm	Th/ppm	Th/U	Pb/ppm	207/206-4	+/-	208/206-4	+/-	207/235-4	+/-	206/238-4	+/-	% conc	Age 206/238	+/-	Age 207/235	+/-	Age 207/206	+/-
om32-14-2a	oz,sp	322	24	0.076	28	0.0585	0.0008	0.0218	0.0015	0.7578	0.0197	0.0939	0.0020	105	579	12	573	11	549	28
om32-14-3a	oc,oz,hl	65	33	0.500	41	0.1985	0.0010	0.1380	0.0016	14.8606	0.3422	0.5429	0.0118	99	2,796	49	2,806	22	2,814	9
om32-14-3b	oc,oz,hl,sp	92	43	0.466	53	0.1980	0.0009	0.1284	0.0013	13.8725	0.3095	0.5082	0.0108	94	2,649	46	2,741	21	2,810	7
om32-16-1a	sl,sp	18	20	1.120	7	0.1036	0.0055	0.3358	0.0132	4.0840	0.2544	0.2859	0.0075	96	1,621	38	1,651	51	1,690	99
om32-17-1a	oz	643	254	0.395	61	0.0580	0.0007	0.1263	0.0017	0.7387	0.0187	0.0923	0.0019	107	569	11	562	11	530	26
om32-17-1b	oz,sp	581	152	0.261	44	0.0516	0.0013	0.0748	0.0029	0.5453	0.0207	0.0766	0.0020	177	476	12	442	14	269	56
om32-19-1a	oz,sp	124	81	0.649	13	0.0529	0.0022	0.1848	0.0055	0.6761	0.0334	0.0927	0.0020	177	572	12	524	20	323	95
om32-21-1a	oz	468	183	0.391	45	0.0581	0.0008	0.1158	0.0019	0.7569	0.0198	0.0945	0.0020	109	582	12	572	11	532	29
om32-21-1b	oz,lp	1,294	394	0.304	120	0.0582	0.0006	0.0922	0.0013	0.7377	0.0175	0.0919	0.0019	105	567	11	561	10	538	21
om32-23-1a	oc,oz,sp	388	226	0.583	188	0.1535	0.0006	0.1648	0.0007	9.0420	0.1957	0.4272	0.0089	96	2,293	40	2,342	20	2,385	7
om32-23-3a	oz,sp	3,478	280	0.081	294	0.0587	0.0002	0.0242	0.0002	0.7350	0.0155	0.0909	0.0019	101	561	11	559	9	554	6
om32-24-1a	c,oz,sp	198	116	0.583	20	0.0595	0.0018	0.1788	0.0046	0.7696	0.0305	0.0939	0.0020	99	578	12	580	18	584	66
om32-24-3a	c,sz,sp	168	75	0.446	16	0.0614	0.0017	0.1387	0.0040	0.7735	0.0285	0.0914	0.0020	86	564	12	582	16	652	58
om32-24-4a	c,il	149	81	0.544	87	0.1852	0.0014	0.1461	0.0012	13.0550	0.3100	0.5113	0.0110	99	2,662	47	2,684	22	2,700	13
om32-24-4b	c,il,sp	352	55	0.156	103	0.1284	0.0005	0.0463	0.0007	5.1009	0.1116	0.2881	0.0060	79	1,632	30	1,836	19	2,076	7
om32-24-6a	wl,sz	239	100	0.417	22	0.0605	0.0013	0.1278	0.0030	0.7671	0.0242	0.0919	0.0020	91	567	12	578	14	623	45
om32-26-1a	r,oz	1,607	456	0.284	144	0.0580	0.0004	0.0852	0.0009	0.7271	0.0167	0.0909	0.0019	106	561	11	555	10	530	16
om32-28-a	oz	123	73	0.595	13	0.0597	0.0034	0.1822	0.0083	0.7486	0.0471	0.0910	0.0020	95	561	12	567	27	593	122
om32-28-b	oz	109	53	0.488	10	0.0593	0.0031	0.1505	0.0075	0.7361	0.0433	0.0901	0.0020	96	556	12	560	25	577	112
om32-28-c	oz	173	44	0.255	15	0.0587	0.0017	0.0750	0.0039	0.7277	0.0275	0.0900	0.0020	100	555	12	555	16	555	62
om32-28-d	oz,lp	115	46	0.400	11	0.0558	0.0028	0.1165	0.0067	0.6795	0.0390	0.0883	0.0020	123	546	12	526	24	444	112
U-rich OM-3-2 subgroup with weak luminescence																				
om32-14-4a	il,sp	1,849	788	0.426	178	0.0588	0.0002	0.1272	0.0006	0.7640	0.0164	0.0942	0.0019	104	580	11	576	9	560	9
om32-16-2a	wil,ro	2,736	380	0.139	132	0.0548	0.0008	0.0252	0.0019	0.3606	0.0096	0.0478	0.0010	75	301	6	313	7	402	33
om32-16-2b	wil,ro	2,402	134	0.056	123	0.0538	0.0007	0.0158	0.0017	0.3864	0.0100	0.0521	0.0011	90	327	7	332	7	363	30
om32-17-2a	wil,ro	2,224	135	0.061	142	0.0573	0.0008	0.0316	0.0017	0.5161	0.0136	0.0653	0.0014	81	408	8	423	9	504	29
om32-21-2a	wl,ro	1,134	330	0.291	103	0.0584	0.0004	0.0923	0.0009	0.7350	0.0165	0.0912	0.0019	103	563	11	559	10	546	15
om32-21-3a	wl,ro	3,203	1,264	0.395	279	0.0581	0.0005	0.1095	0.0011	0.6633	0.0153	0.0828	0.0017	96	513	10	517	9	533	18
om32-23-2a	wl	1,779	515	0.289	130	0.0570	0.0003	0.1133	0.0007	0.5709	0.0124	0.0726	0.0015	92	452	9	459	8	492	11
om32-23-2b	wl	1,354	579	0.427	128	0.0588	0.0003	0.1294	0.0008	0.7454	0.0165	0.0920	0.0019	102	567	11	566	10	558	12
om32-23-4a	wl	839	415	0.495	79	0.0588	0.0005	0.1543	0.0012	0.7265	0.0168	0.0896	0.0019	99	553	11	554	10	559	18
om32-24-2a	wil,ro	2,804	156	0.056	171	0.0533	0.0011	0.0227	0.0027	0.4448	0.0140	0.0606	0.0013	111	379	8	374	10	340	48
om32-24-5a	wil,ro	2,679	445	0.166	210	0.0581	0.0005	0.0580	0.0011	0.6363	0.0147	0.0795	0.0016	93	493	10	500	9	533	18
om32-24-7a	wil	2,046	420	0.205	134	0.0550	0.0004	0.0883	0.0010	0.5015	0.0115	0.0662	0.0014	101	413	8	413	8	411	18
om32-24-7b	wil,sp	3,050	1,325	0.434	257	0.0579	0.0003	0.1773	0.0010	0.6302	0.0138	0.0790	0.0016	93	490	10	496	9	525	11
om32-26-2a	wil,ro	2,664	311	0.117	179	0.0567	0.0007	0.0281	0.0015	0.5295	0.0131	0.0678	0.0014	88	423	8	431	9	479	25
om32-27-1a	wil	4,110	435	0.106	249	0.0545	0.0008	0.0303	0.0018	0.4386	0.0116	0.0584	0.0012	94	366	7	369	8	391	31
om32-27-1b	wil	2,466	469	0.190	205	0.0566	0.0004	0.0607	0.0010	0.6576	0.0151	0.0843	0.0017	110	522	10	513	9	476	17
om32-27-1c	wil,sp	3,788	835	0.220	287	0.0545	0.0009	0.0603	0.0022	0.5008	0.0141	0.0667	0.0014	107	416	8	412	10	390	38
Sample SB-22. "unit 2"																				
sb22-1-6a	c,wl,ro	3,641	2,011	0.552	375	0.0598	0.0002	0.1680	0.0006	0.8006	0.0095	0.0972	0.0010	100	598	6	597	5	595	9
sb22-2-1a	c,sl	177	59	0.336	14	0.0514	0.0031	0.0885	0.0075	0.5457	0.0348	0.0770	0.0010	186	478	6	442	23	257	140
sb22-2-1b	r,oz,sp	1,853	351	0.189	135	0.0563	0.0004	0.0551	0.0008	0.5898	0.0078	0.0759	0.0008	101	472	5	471	5	465	14
sb22-2-2a	oz	567	183	0.323	52	0.0575	0.0008	0.0955	0.0018	0.7295	0.0136	0.0921	0.0010	111	568	6	556	8	509	30
sb22-2-2b	il,sp	775	188	0.242	54	0.0547	0.0011	0.0144	0.0026	0.5504	0.0137	0.0729	0.0008	113	454	5	445	9	402	47
sb22-2-3a	c,oz	865	491	0.568	81	0.0583	0.0006	0.1793	0.0016	0.7061	0.0115	0.0878	0.0010	100	543	6	542	7	542	23
sb22-2-3b	oc,oz	407	137	0.337	37	0.0575	0.0011	0.1010	0.0026	0.7115	0.0168	0.0897	0.0010	108	554	6	546	10	511	42
sb22-2-3c	r,oz,lp	523	205	0.392	40	0.0547	0.0014	0.1088	0.0033	0.5550	0.0162	0.0736	0.0008	115	458	5	448	11	399	57

sb22-3-1a	c,il,ro	784	164	0.209	82	0.0604	0.0005	0.0634	0.0010	0.8958	0.0132	0.1076	0.0012	107	659	7	649	7	618	19
sb22-3-2a	oz	246	146	0.593	19	0.0529	0.0022	0.1727	0.0054	0.5277	0.0233	0.0723	0.0009	138	450	5	430	15	326	93
sb22-3-2b	oz,sp	578	213	0.368	42	0.0544	0.0011	0.1068	0.0027	0.5408	0.0136	0.0721	0.0008	116	449	5	439	9	387	47
sb22-3-3a	c,sz,sp	171	182	1.064	20	0.0574	0.0019	0.3192	0.0053	0.7564	0.0281	0.0957	0.0012	117	589	7	572	16	505	73
sb22-5-1a	c,sl	63	22	0.354	9	0.0712	0.0038	0.1249	0.0091	1.3027	0.0753	0.1326	0.0020	83	803	12	847	33	964	110
sb22-5-1b	r,oz,lp	486	22	0.045	45	0.0567	0.0009	0.0093	0.0020	0.7806	0.0165	0.0998	0.0011	127	613	7	586	9	482	36
sb22-5-2a	oc,wl	584	282	0.484	315	0.1843	0.0006	0.1314	0.0006	12.1218	0.1424	0.4769	0.0052	93	2,514	23	2,614	11	2,692	5
sb22-5-2b	oc,wl	600	345	0.576	270	0.1584	0.0005	0.1565	0.0007	8.6750	0.1026	0.3972	0.0044	88	2,156	20	2,304	11	2,439	5
sb22-5-2c	r,oz,sp	168	5	0.027	9	0.0511	0.0022	0.0115	0.0049	0.4203	0.0192	0.0597	0.0008	153	374	5	356	14	245	97
sb22-5-3a	c,wl	1,432	188	0.131	129	0.0593	0.0004	0.0384	0.0008	0.7780	0.0105	0.0951	0.0010	101	586	6	584	6	579	15
sb22-9-1a	wl	2,263	2,692	1.190	398	0.0485	0.0056	0.0809	0.0138	0.4453	0.0528	0.0666	0.0008	332	415	5	374	37	125	253
sb22-11-1a	oz	280	105	0.376	67	0.1001	0.0008	0.1152	0.0017	3.1033	0.0463	0.2248	0.0026	80	1,307	14	1,434	11	1,626	15
sb22-11-1b	oz	249	58	0.233	31	0.0816	0.0014	0.0790	0.0029	1.3668	0.0298	0.1215	0.0015	60	739	8	875	13	1,235	33
sb22-11-1c	oz,sp	1,061	397	0.374	83	0.0560	0.0007	0.1127	0.0016	0.5945	0.0102	0.0770	0.0008	106	478	5	474	6	451	26
sb22-11-2a	c,sz	137	53	0.390	14	0.0569	0.0027	0.1052	0.0064	0.7661	0.0384	0.0976	0.0013	123	600	8	578	22	488	103
sb22-11-2b	r,il,sp	560	157	0.281	43	0.0585	0.0010	0.0965	0.0023	0.6275	0.0136	0.0778	0.0009	88	483	5	495	8	548	37
sb22-13-1a	wil	2,545	56	0.022	161	0.0552	0.0006	0.0050	0.0013	0.5157	0.0085	0.0677	0.0007	100	423	5	422	6	421	25
sb22-13-3a	oc,oz	119	52	0.437	9	0.0551	0.0035	0.1300	0.0084	0.5617	0.0370	0.0740	0.0011	111	460	6	453	24	415	140
sb22-13-3b	oc,oz	102	39	0.383	8	0.0528	0.0050	0.1162	0.0121	0.5400	0.0532	0.0741	0.0011	143	461	7	438	35	322	217
sb22-13-3c	r,oz,sp	683	76	0.111	44	0.0535	0.0028	0.0361	0.0068	0.4265	0.0237	0.0578	0.0007	103	362	4	361	17	351	120
sb22-13-2a	oc,sz	39	23	0.592	4	0.0631	0.0054	0.2024	0.0134	0.8702	0.0779	0.1001	0.0016	86	615	9	636	42	711	184
sb22-13-2b	oc,il	537	20	0.036	36	0.0636	0.0027	0.0322	0.0061	0.5933	0.0266	0.0677	0.0008	58	422	5	473	17	728	89
sb22-13-2c	r,wl,sp	573	19	0.033	29	0.0523	0.0015	0.0078	0.0034	0.3922	0.0126	0.0544	0.0006	114	341	4	336	9	298	65
Sample 91-1c. “unit 3”																				
91-3-1a	wil	3,105	359	0.116	231	0.0575	0.0003	0.0408	0.0005	0.6227	0.0100	0.0785	0.0012	95	487	7	492	6	512	10
91-3-1b	wil,sp	4,201	857	0.204	319	0.0571	0.0002	0.0743	0.0004	0.6112	0.0096	0.0777	0.0012	98	482	7	484	6	493	8
91-3-2a	oc,oz	540	388	0.718	51	0.0544	0.0013	0.2180	0.0035	0.6312	0.0193	0.0842	0.0013	135	521	8	497	12	386	55
91-3-2b	oz,wl,sp	1,597	17	0.011	77	0.0537	0.0005	0.0052	0.0009	0.3934	0.0071	0.0531	0.0008	93	334	5	337	5	359	19
91-6-1a	r,wil,sp	2,102	20	0.009	101	0.0535	0.0005	0.0034	0.0008	0.3905	0.0071	0.0529	0.0008	94	332	5	335	5	352	19
91-6-1b	c,wil	1,281	301	0.235	76	0.0545	0.0006	0.0759	0.0015	0.4580	0.0092	0.0610	0.0009	98	382	6	383	6	390	26
91-6-1c	r,wil,sp	1,576	15	0.009	77	0.0529	0.0006	0.0019	0.0011	0.3916	0.0075	0.0537	0.0008	103	337	5	336	6	326	24
91-6-2a	oz	181	104	0.573	72	0.2098	0.0012	0.1777	0.0020	9.6197	0.1669	0.3325	0.0052	64	1,851	25	2,399	16	2,904	9
91-6-2b	oz,lp	264	138	0.522	162	0.2109	0.0007	0.1536	0.0009	15.1488	0.2439	0.5209	0.0080	93	2,703	34	2,825	15	2,912	5
91-6-3a	oz,ro	226	91	0.402	20	0.0568	0.0020	0.1223	0.0048	0.6814	0.0275	0.0869	0.0014	111	537	8	528	17	485	77
91-6-4a	oz	426	223	0.524	76	0.1375	0.0008	0.1682	0.0015	2.9996	0.0506	0.1582	0.0024	43	947	13	1,408	13	2,196	10
91-6-4b	oz,lp	603	308	0.512	211	0.1276	0.0005	0.1430	0.0009	5.6153	0.0892	0.3191	0.0048	86	1,785	23	1,918	14	2,065	6
91-6-5a	c,oz	186	128	0.689	20	0.0580	0.0020	0.2129	0.0052	0.7830	0.0317	0.0979	0.0016	113	602	9	587	18	531	77
91-6-5b	r,il,sp	514	9	0.018	27	0.0526	0.0013	0.0003	0.0028	0.4163	0.0126	0.0574	0.0009	115	359	5	353	9	314	55
91-7-1a	r,wl,sp	775	19	0.025	38	0.0524	0.0009	0.0056	0.0020	0.3826	0.0096	0.0529	0.0008	109	332	5	329	7	305	41
91-7-1b	oc,wil	922	100	0.108	69	0.0571	0.0006	0.0349	0.0014	0.6214	0.0123	0.0789	0.0012	99	490	7	491	8	496	24
91-7-1c	r,wl,sp	921	24	0.027	46	0.0506	0.0011	0.0038	0.0025	0.3767	0.0106	0.0540	0.0008	152	339	5	325	8	224	50
91-7-2a	oc,oz	23	31	1.357	3	0.0477	0.0158	0.3809	0.0400	0.6070	0.2042	0.0923	0.0028	666	569	17	482	130	85	639
91-7-2b	oc,oz,sp	104	180	1.727	14	0.0584	0.0034	0.5397	0.0099	0.7451	0.0464	0.0925	0.0016	104	570	10	565	27	546	126
91-7-3a	wil,ro	726	13	0.018	35	0.0537	0.0014	0.0066	0.0031	0.3856	0.0121	0.0521	0.0008	91	327	5	331	9	358	58
91-10-1a	wil	2,316	61	0.026	113	0.0532	0.0004	0.0075	0.0008	0.3901	0.0068	0.0532	0.0008	99	334	5	334	5	338	17
91-10-1b	wil,sp	1,339	34	0.025	65	0.0513	0.0008	0.0036	0.0017	0.3722	0.0084	0.0526	0.0008	129	330	5	321	6	255	34
91-10-2a	wil	4,656	2,893	0.621	456	0.0589	0.0002	0.1967	0.0005	0.7354	0.0113	0.0905	0.0013	99	559	8	560	7	564	6
91-10-2b	wil,ro	4,088	2,170	0.531	367	0.0578	0.0002	0.1739	0.0006	0.6720	0.0105	0.0843	0.0012	100	522	7	522	6	522	8
91-11-1a	c,oz,ro	320	133	0.417	28	0.0569	0.0013	0.1415	0.0033	0.6503	0.0195	0.0829	0.0013	106	514	8	509	12	486	52
91-12-1a	c,sz	209	76	0.363	20	0.0586	0.0016	0.1108	0.0037	0.7606	0.0250	0.0942	0.0015	105	580	9	574	14	551	58

Table 1 (contd.)

Spot	Comment	U/ppm	Th/ppm	Th/U	Pb/ppm	207/206-4	+/-	208/206-4	+/-	207/235-4	+/-	206/238-4	+/-	% conc	Age 206/238	+/-	Age 207/235	+/-	Age 207/206	+/-
91-12-1b	r,wil,ro	384	28	0.074	27	0.0573	0.0017	0.0230	0.0040	0.5808	0.0205	0.0735	0.0011	91	457	7	465	13	502	66
91-12-2a	c,sz	53	52	0.978	30	0.1587	0.0018	0.2690	0.0039	9.8931	0.2206	0.4522	0.0080	99	2,405	36	2,425	21	2,442	19
91-12-2b	c,sz	62	59	0.949	28	0.1567	0.0020	0.2790	0.0046	7.7524	0.1784	0.3588	0.0063	82	1,977	30	2,203	21	2,420	22
91-12-2c	c,sz,ro	54	45	0.843	27	0.1578	0.0020	0.2421	0.0043	9.1378	0.2105	0.4200	0.0075	93	2,260	34	2,352	21	2,432	21
91-12-3a	oz,ro	377	138	0.365	29	0.0582	0.0012	0.1201	0.0029	0.6064	0.0168	0.0756	0.0012	87	470	7	481	11	537	46
91-12-4a	il	736	619	0.841	72	0.0593	0.0009	0.2944	0.0026	0.6737	0.0156	0.0825	0.0013	89	511	7	523	9	576	34
91-12-4b	il,sp	600	219	0.365	48	0.0595	0.0015	0.1074	0.0036	0.6221	0.0191	0.0758	0.0012	80	471	7	491	12	587	54
91-12-5a	c,oz	354	119	0.336	26	0.0550	0.0018	0.1083	0.0043	0.5283	0.0200	0.0697	0.0011	105	434	7	431	13	412	73
91-12-5b	c,oz,sp	742	379	0.510	59	0.0563	0.0009	0.1681	0.0023	0.5763	0.0135	0.0742	0.0011	99	461	7	462	9	465	35
91-15-1a	c,oz,ro	269	213	0.792	29	0.0593	0.0019	0.2546	0.0050	0.7501	0.0286	0.0918	0.0015	98	566	9	568	17	577	71
91-15-2a	c,sl,sp	22	2	0.107	3	0.0864	0.0151	-0.0427	0.0345	1.2371	0.2232	0.1039	0.0030	47	637	17	818	102	1,346	343
91-16-1a	oz	489	58	0.119	29	0.0538	0.0013	0.0348	0.0029	0.4614	0.0137	0.0622	0.0010	107	389	6	385	10	364	53
91-16-1b	oz,lp	311	67	0.214	19	0.0554	0.0021	0.0707	0.0050	0.4779	0.0204	0.0626	0.0010	92	392	6	397	14	427	84
91-16-2a	wl	1,494	20	0.013	73	0.0537	0.0005	0.0061	0.0009	0.3958	0.0073	0.0534	0.0008	93	335	5	339	5	360	20
91-16-2b	wl,sp	1,883	31	0.017	92	0.0530	0.0005	0.0047	0.0010	0.3898	0.0072	0.0534	0.0008	102	335	5	334	5	327	21
91-16-3a	c,sl,ro	28	30	1.070	11	0.1654	0.0037	0.4304	0.0093	6.2939	0.2056	0.2760	0.0058	63	1,571	29	2,018	29	2,511	38
91-16-4a	c,il,sp	270	221	0.818	86	0.1191	0.0008	0.2518	0.0018	4.4326	0.0772	0.2699	0.0042	79	1,540	21	1,718	14	1,943	12

margins. This is typical for zircon which has experienced high-grade metamorphic conditions (e.g. Pidgeon 1992; Nemchin and Pidgeon 1997; Pidgeon et al. 1998; Schaltegger et al. 1999; Hoskin and Black 2000), either in the source environments of the detrital zircons, or due to the tectonometamorphic events which effected the consolidating sediments.

CL images on Fig. 3 show that zircons from the different units display similar features. Most evident is the presence of euhedral to subhedral fine, oscillatory zoned zircon in samples St-4-1 (grain 20) from CSGC Unit 1 and OM-3-2 (grains 28, 14-1) from the OGC. Also common to these samples are rounded nebulously zoned zircons consisting of central dark grey (CL) domains surrounded by outer lighter CL mantles (e.g. St-4-1:18, 17-1 and OM-3-2: 14-4). Also present in these populations are minor, irregularly shaped, high U-Th, spongy CL textured grains (St-4-1, 16-1: OM-3-2, 24-2). Zircons from sample SB-22 (CSGC Unit 2) have irregular, embayed shapes and are finely oscillatory zoned with some zonal thickening (grain 2-3). Also present are subhedral, dark-centered (CL) nebulously zoned zircon (e.g. SB-22, grain 2-3) sometimes with curved zones (SB-22, grain 13-2). An important feature of this population is that grains frequently show metamorphic overgrowths concentrated at crystal terminations (e.g. SB-22: grains 13-2, 13-3 and 5-2). Zircons from sample 91-1c from Unit 3 have irregular to rounded oscillatory zoning (e.g. 16-1 and 6-2) but also contain more complex grains showing cores and metamorphic rims (grains 3-2, 6-1, 12-1 and 12-3), subdued sector zoning (7-2), and unzoned grains (under CL) with marginal overgrowth or recrystallisation (grain 16-2).

SHRIMP zircon age results

Sample St-4-1 (CSGC Unit 1)

SHRIMP results in Table 1 show that most analyses on euhedral fine, partially recrystallized oscillatory zoned, and irregular-shaped nebulously zoned zircon give $^{206}Pb/^{238}U$ ages in the range 0.65–0.55 Ga, corresponding to the Neoproterozoic. The consistency of these ages within and between grains (e.g. 19-2, 20-2, 20-3, 22-1, 24-1) strongly supports an episode of multiple igneous and metamorphic events in the Neoproterozoic. On the concordia plot (Fig. 2) the main body of data points is seen to fall along concordia between 600 and 550 Ma with some points extending down to ca. 400 Ma. This suggests that a number of zircons have experienced minor, unsystematic isotopic disturbances during Variscan metamorphism, limiting our ability to make a precise analysis of the age structure of Neoproterozoic events. Evidence for a Variscan overprint may be provided by $^{206}Pb/^{238}U$ age values of 400–430 Ma, observed for one grain (St-4-1, grain 16, Table 1). This grain has the highest measured U content of all grains analyzed (2,500 ppm) and has a uniform, nebulously zoned, spongy structure (Fig. 3) suggesting that the grain has enhanced radiation damage and was

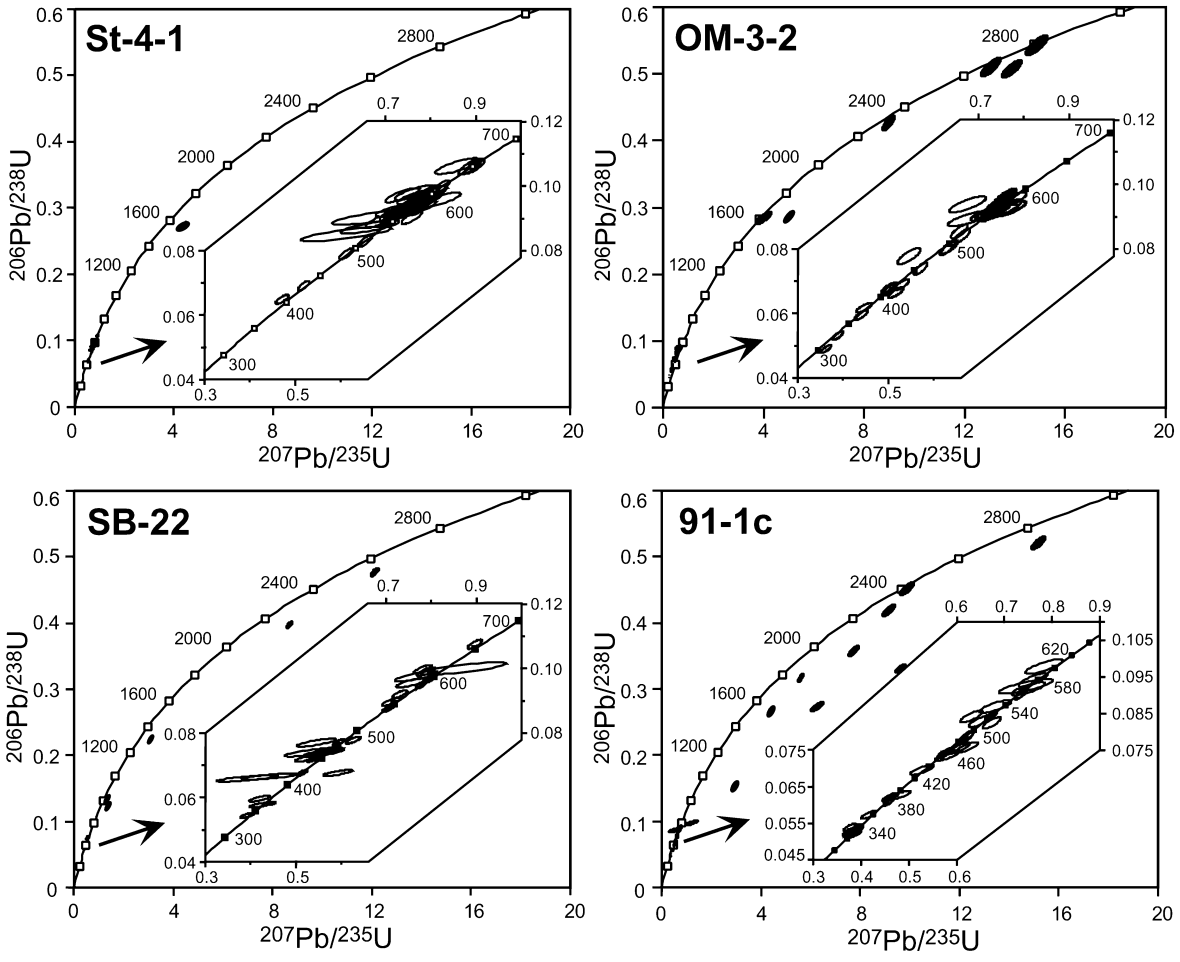

Fig. 2 Concordia diagrams displaying SHRIMP data corrected for common Pb (using the ^{204}Pb concentration). *Errors* are plotted on the 1 sigma standard deviation level

partially reset during Variscan metamorphism. This event also appears to have influenced grain 22. This grain has a euhedral, low U-Th, high CL centre with high U-Th, low CL zircon, concentrated at the terminations. Analysis 2b, with the highest U content of ca. 2,000 ppm, records a significant loss of radiogenic Pb during the Variscan event.

The oldest phase found is an oscillatory zoned and partly transgressively recrystallized core in grain 23-1 with a ^{207}Pb/^{206}Pb-age of about 1.9 Ga indicating a Palaeoproterozoic (Eburnian) minimum age. This core is surrounded by nebulously zoned metamorphic zircon corresponding in age (^{206}Pb/^{238}U age: 0.65 Ga) to the major Neoproterozoic event(s) recorded by most zircons.

Sample OM-3-2 (OGC)

The abundance of high U grains is a marked difference between the zircons from this and the previous sample. Also, old zircons are more abundant in this sample, with ^{207}Pb/^{206}Pb ages ranging from about 1.7 to 2.8 Ga, mostly with only minor discordance. The late Archean/Early Proterozoic subpopulation consists of low U-Th zircons with patchy zoning, and in the case of grain 14-3, a uniform grey CL overgrowth (Fig. 3). One strongly luminescent grain has very low U-Th concentrations of about 20 ppm (grain 16-1), resulting in large uncertainty in the U-Pb ages.

The main group of zircons has Neoproterozoic ages, very similar to sample St-4-1. One subpopulation displays well-preserved primary oscillatory zoning, with only local non-planar textures or blurring (cf. Hoskin and Black 2000; e.g. grains 14-1 and 28, Fig. 3) and with a spread of ^{206}Pb/^{238}U ages of 0.59–0.55 Ga. On the concordia diagram, this main population shows a concentration of data points at about 580 Ma, and a spread of data points along concordia to approximately 300 Ma. From Table 1 it can be seen that zircon areas with lower ages also have the highest U-Th contents (i.e. grains 14-4, 16-2, 17-2, 21-2, 21-3, 23-2, 23-4, 24-2, 24-5, 24-7, 26-2, 27-1). Probably, lattice breakdown to the metamict state and Variscan recrystallization (e.g. grain 24-2, Fig. 3) enhanced partial or complete resetting of the primary Neoproterozoic U-Pb isotope systems during Carboniferous metamorphism. As a consequence, the highest ^{206}Pb/^{238}U age found in this subpopulation provides a minimum estimate of the age of primary crystallization (0.58 Ga). The lowest ^{206}Pb/^{238}U age of

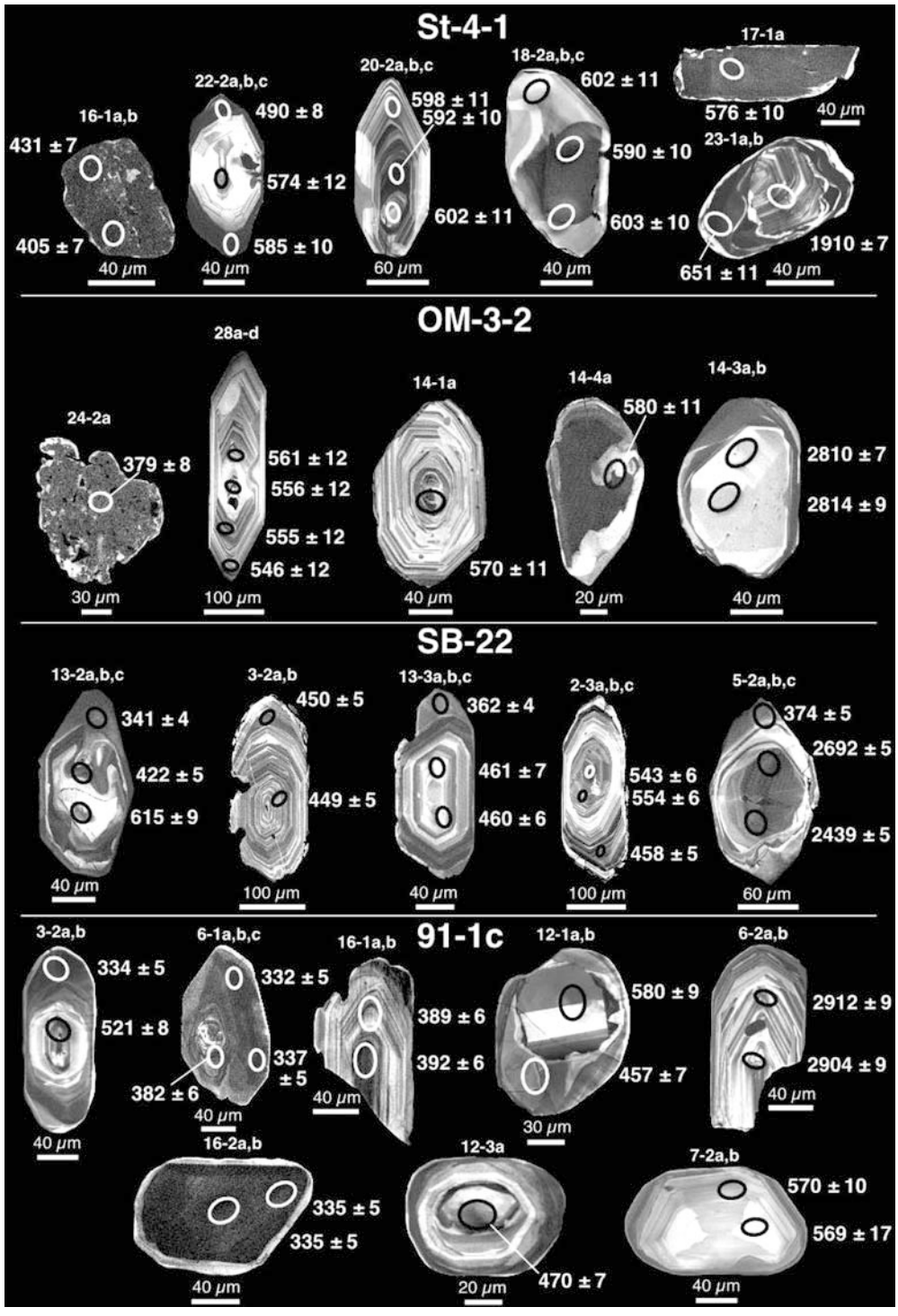

Fig. 3 Cathodoluminescence images and SHRIMP spot analyses of selected zircon grains from four high-grade metasedimentary rocks from different tectonometamorphic units of the CSGC and from the OGC. Samples *St-4-1*, *OM-3-2* and *SB-22* are LP-HT metamorphic rocks; sample *91-1c* is a granulite-facies rock. Ages are calculated from the $^{238}U/^{206}Pb$ ratios for Paleozoic and Neoproterozoic zircon, and from $^{207}Pb/^{206}Pb$ ratios for Archean/Palaeoproterozoic zircon

about 0.3 Ga demonstrates the significant influence of the Carboniferous metamorphic event on the zircon population from this sample.

Sample SB-22 (CSGC Unit 2)

The zircon U-Pb systems have similar age components to those in the previous samples (Table 1). However, the zircons with highest $^{207}Pb/^{206}Pb$ ages in SB-22 are strongly discordant (e.g. grain 5-2) compared to old cores in zircons from the previous samples. Nevertheless, the $^{207}Pb/^{206}Pb$ ages support Early Proterozoic or even late Archean zircon generation. As in the previous samples, an important Neoproterozoic subpopulation ($^{206}Pb/^{238}U$ ages: 0.65–0.55 Ga) is present (Fig. 2). Besides these Neoproterozoic components a number of grains have $^{206}Pb/^{238}U$ ages in the range of 0.48–0.45 Ga

(e.g. grains 2-3, 3-2, 13-3 in Fig. 3). Some oscillatory zoned grains (e.g. grain 3-2) are uniformly of this age. Others have significantly younger, unzoned overgrowths (e.g. grain 13-3), and some consist of an older 0.55 Ga core surrounded by a 0.45 Ga oscillatory zoned rim. These relationships, clearly indicated on Fig. 3, together with the observed age peak at ca 0.45 Ga (Fig. 2) and the association of oscillatory zoning with the 0.48–0.45 Ga ages, are taken as evidence for an important zircon-generating igneous event at this time. Such a late Ordovician detrital component was not observed in the previous samples. The presence of weakly zoned zircon terminations (e.g. grains 13-2, 13-3) with $^{206}Pb/^{238}U$ ages of 0.43–0.34 Ga is attributed to overgrowths or recrystallisation during Variscan metamorphism.

Sample 91-1c (CSGC Unit 3)

Many grains of this sample are rounded and complex. The zircons have a wide range of U and Th contents indicating variable conditions of formation. A number of older zircons are present, which are generally highly discordant (Fig. 2, Table 1) but have Late Archean to Early Proterozoic $^{207}Pb/^{206}Pb$ ages (2.9–1.9 Ga). These are interpreted as minimum ages for zircon crystallization in igneous environments (e.g. grain 6-2). Neoproterozoic $^{206}Pb/^{238}U$ age values (0.60–0.56 Ga) are restricted to zircon cores where primary zoning appears as weak sector zoning (e.g. grain 7-2). The 0.60 Ga cores are surrounded by nebulously zoned ca. 0.46 Ga rims (e.g. grain 12-1) and in some grains by Carboniferous terminations (e.g. grain 3-2). On the concordia plot data points are seen to extend along concordia from ca 600 to 340 Ma. This spread is attributed to partial disturbance of the U-Pb systems during the Carboniferous granulite-facies metamorphism (e.g. grain 3-2). There are, however, detrital components in this population which clearly have been generated during Palaeozoic times (0.49–0.46 Ga). Similar to SB-22 (e.g. grain 13-3) they occur either as cores (e.g. grains 7-1, 12-5 in Table 1) or as monophases with partly preserved primary oscillatory zoning, concordancy of the U-Pb system, and good reproducibility of the $^{206}Pb/^{238}U$ ages (e.g. grain 3-1 in Table 1). One grain was found to have a Devonian age (0.39 Ga, grain 16-1). Two spot analyses on this grain which has well developed oscillatory zoning but a very irregular crystal shape gave identical results within the error limits. This grain is the youngest detrital component found in sample 91-1c. A similar $^{206}Pb/^{238}U$ age was also found in a concordant core area of grain 6-1 whose weakly luminescent oscillatory zoning appears strongly blurred due to recrystallization which probably occurred during the formation of the thick Carboniferous rim on this grain.

A further subpopulation of zircon was observed in this rock which has been generated in the course of the Carboniferous granulite-facies event. These occur as either euhedral and rather homogeneous grains with weak luminescence (grains 7-3, 10-1, 16-2), or as rims around significantly older cores (grains 3-2, 6-1, 6-5, 7-1). The average $^{206}Pb/^{238}U$ ratios of zircon areas with concordant U-Pb isotope systems give an age value of 335 ± 2 Ma (1 standard deviation). This is a precise estimate of the time of zircon crystallization, triggered by the granulite-facies metamorphic event of Unit 3. It agrees with the age estimate of Hanel et al. (1993) using single zircon and the Pb evaporation method. High-grade metamorphic growth of this subpopulation is in agreement with the low Th/U ratios of the grains (0.01–0.03, Table 1) which has been reported to be a feature of granulite facies metamorphic zircons ($Th/U < 0.07$: Rubatto 2002). An identical age of granulite-facies metamorphism was reported by Schaltegger et al. (1999) for rocks of the Vosges basement, which are of igneous and sedimentary origin. Zircons from these samples show internal morphologies very similar to 91-1c, with Neoproterozoic relic phases and irregular weakly luminescing 335 Ma metamorphic rims.

Discussion of general trends

The extended distribution of the data points as a whole on the concordia plot (Fig. 2) can be explained either by the presence of zircons from different source regions with complex age patterns, respectively, by the partial isotopic disturbance of zircons with a uniform age by later metamorphic events or by a combination of both. The consistency of U-Pb ages within individual grains argues more for the first case. Repeated spot analyses on the same grain in many cases yield reproducible age values (e.g. grains St-4-1-20-2, St-4-1-18-2, OM-3-2-28, 91-1c-6-2, 91-1c-7-2: Fig. 3). This demonstrates that the U-Pb systems in the detrital zircons have in many cases remained closed under conditions of up to granulite-facies. The ages recorded in these grains should thus be significant in characterizing the sediment sources and estimating times of sedimentation. Zircon areas that show ages intermediate between events in the sediment sources and Variscan metamorphism are generally high in U and/or Th suggesting that these zircons were more susceptible to isotopic disturbance during later events. The generally good preservation of original age information in the detritus is in accordance with mostly well-preserved crystal shapes and surfaces of the detrital individuals. This suggests generally short distances of sediment transport and close spatial relations between the marine sediment basins and the eroding hinterlands.

All four investigated metasedimentary zircon populations are obviously dominated by Precambrian components which were generated during either late Archean/Palaeoproterozoic or Neoproterozoic events. There is no zircon phase which can be clearly attributed to a Mesoproterozoic episode, such as for example the Grenvillian zircons reported from the Bohemian Massif or the Mid-German Crystalline Rise (Gebauer et al. 1989; Zeh et al. 2001; Linnemann et al. 2000;

Hegner et al. 2000; Friedl et al. 2000). This 'Mesoproterozoic gap' is typical for Gondwana sediment sources such as for example the West Africa Craton (WAC; e.g. Rocci et al. 1991; Nance and Murphy 1996).

There is a general lack of Cambrian and Early Ordovician zircon phases in the Schwarzwald metasediments, apart from a few spot analyses on zircons from population 91-1c which are interpreted to have been partially reset by the strong Carboniferous metamorphic overprint of Neoproterozoic zircon. Younger pre-Carboniferous zircon phases are rare in the Schwarzwald detritus. Only two of the analyzed samples (SB-22, 91-1c) contain detrital subpopulations with late-Ordovician/Silurian ages, and only in rock 91-1c has rare Devonian zircon been found (Fig. 4). The detritus age patterns indicate a specific history of pre-Variscan deposition for the four studied metasediment samples and rule out transfer of detritus from one common source area in a single sedimentation cycle. On the other hand all the studied sediments carry detrital zircons with ages ≤ 550 Ma. This suggests that the protoliths were deposited during **Palaeozoic** sedimentation episodes.

The influence of the Variscan metamorphic event(s) is most strongly recognized in U, Th rich zircons whose CL images indicate a high degree of metamictization and metamorphic recrystallization of the disturbed zircon lattices. Together with the mostly well-preserved crystal shapes of the zircons as a whole the rare occurrence of Variscan zircon indicates that under the given maximum P–T conditions at 330 Ma (about 750 °C, 0.42–0.45 GPa; Kalt et al. 2000) dissolution of detrital zircon and crystallization of metamorphic zircon was not a predominate phenomenon. Only in 91-1c a significant subpopulation has been found being completely metamorphic and having euhedral shapes. This subpopulation has been generated at considerably higher temperatures of the granulite facies (>950 °C; Marschall et al. 2003).

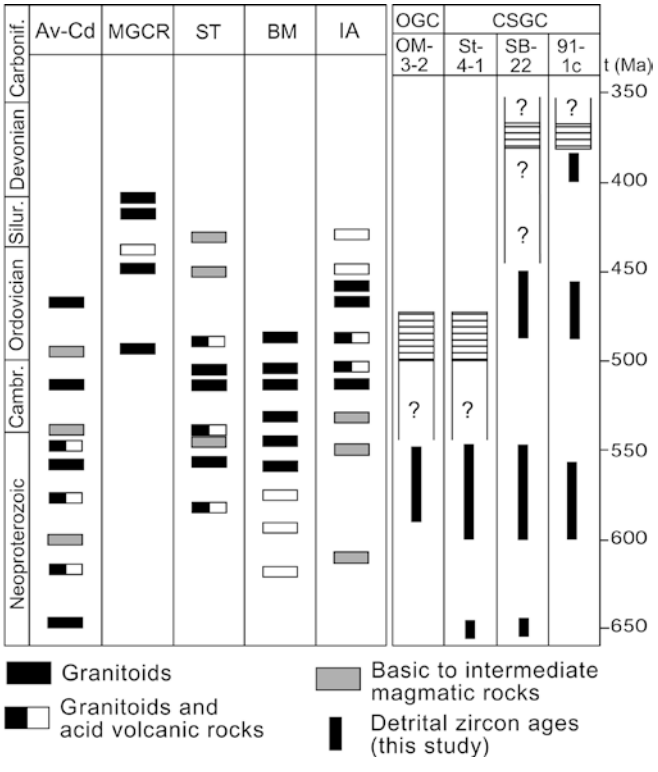

Fig. 4 Comparison of detrital zircon age distributions of the OGC and the CSGC (this study), with zircon data from the literature for the Avalonian-Cadomian (*Av-Cd*) terrane, the Mid-German Crystalline Rise (*MGCR*), the Saxothuringian (*ST*) belt, the Bohemian Massif (*BM*), and the intra-Alpine (*IA*) terranes (modified after von Raumer et al. 2002, with additional data from Anthes and Reischmann 2001 (*MGCR*); Dörr et al. 2002 (*BM*); Eichhorn et al. 2001 (*IA*); Guerrot and Peucat 1990 (*Av-Cd*); Kemnitz et al. 2002 (*ST*); Loth et al. 2001 (*IA*); Reischmann et al. 2001 (*MGCR*); Schaltegger et al. 1997 (*IA*); Schaltegger and Gebauer 1999 (*IA*)). *Hatching* indicates sedimentation episodes determined from the zircon age data of the present study

Constraints on sedimentation episodes and palaeogeographic positions

The history of the investigated metasediments started with an episode of weathering and erosion of Precambrian crust. Different sediment source areas may have to be assumed for the analyzed metasediments. Rare and strongly reworked Eburnian rocks are to be assumed for sample St-4-1, while considerable fractions of only weakly reworked ancient crust must be invoked for other samples (e.g. OM-3-2: various well-preserved rimless Late-Archean/Early Proterozoic zircons). The Neoproterozoic subgroups dominating in all studied metasediments (Fig. 4) are e.g. typical of Morocco/Mauretanian crustal areas (e.g. Söllner et al. 1997). The Neoproterozoic detrital age distributions of the investigated samples show significant differences, in particular due to the presence of ca. 650 Ma components in some samples (Fig. 4). This may suggest a somewhat different orientation of the Early Palaeozoic basin(s) to different types of northern Gondwana hinterlands.

The eroding hinterlands that provided the detritus of all the investigated CSGC and OGC metasediments were obviously subject to the late stages of the polycyclic pan-African event. In the source areas of all the samples studied here, magma generation and metamorphism occurred between ca. 600 and 545 Ma. This fits well to the concept of a Neoproterozoic active margin setting along the entire length of the future Palaeozoic microcontinents at the northern margin of Gondwana (e.g. Tait et al. 1997, 2000; Söllner et al. 1997; Matte 2001; von Raumer et al. 2002; Stampfli et al. 2002 and references therein). In Fig. 4, the ages of detrital zircons from the high-grade metasediments of the OGC and the CSGC are compared to magmatic episodes for the Lower Ordovician microcontinents at the northern margin of Gondwana. While granitoid magmatism at ca. 550 Ma is a widespread feature, older Neoproterozoic ages seem to be a little less common. For the studied

Schwarzwald samples, magmatism and metamorphism in the source regions was obviously terminated at the end of the Neoproterozoic (543 Ma; Bowring et al. 1993; Odin 1994). The prominent Cambrian magmatism characteristic of most terranes is not documented by the detrital zircons in the metasediments, but geochemical data and single zircon dating on orthogneisses have been interpreted to document a Cambrian magmatic arc for the Schwarzwald basement (510–500 Ma; Chen et al. 2000). However, the tectonic and premetamorphic relation between these orthogneisses and the studied metasediments is not clear.

From the Ordovician on, the evolution of the investigated metasediments of the Schwarzwald differed (Fig. 4). No Palaeozoic detrital zircons were found in the metasediments St-4-1 (CSGC Unit 1) and OM-3-2 (OGC). A maximum sedimentation age of about 550 Ma for these samples is given by the youngest detrital zircons. Zeh et al. (2001) suggested that late Proterozoic to Early Cambrian sediments from the Mid German Crystalline Rise, derived from peri-Gondwana, have rather high epsilon-Nd values, while sediments younger than Middle Cambrian commonly have epsilon-Nd (T) values < -6. Liew and Hofmann (1988) reported a value of -7 for a Schwarzwald metasediment close to the location of St-4-1. This could favour an onset of sedimentation in the basins represented by samples St-4-1 and OM-3-2 later than the Middle Cambrian. Hanel et al. (1999) found palynological evidence (chitinozoa) for marine sedimentation of Ordovician age in amphibolite-facies paragneisses from a borehole in the Northern Schwarzwald close to the OGC. A HT event at about 480 Ma, suggested for Unit 1 by various authors on the basis of zircon dating (Steiger et al.1973; Kober et al. 1986), Rb-Sr whole rock data (Hofmann and Köhler 1973) and garnet Pb-Pb dating (Chen et al. 1998, cited in Chen et al. 2000), may be taken as a further argument for Ordovician consolidation of the metasediments of Unit 1 and the OGC. In summary, most of the cited evidence is in favour of a sedimentation episode that started after the Middle Cambrian and terminated in the Ordovician.

In metasediment SB-22 (Unit 2), the presence of a Late Ordovician detrital subpopulation indicates a considerably later episode of erosion and sedimentation for Unit 2 than for Unit 1 sediments. The igneous origin of the youngest (Late Ordovician) detrital zircons evidences melt generation in the source areas, and reworking of Precambrian crust (e.g. grain SB-22-2-3, Fig. 3). The metasediments of Unit 2 contain lenses and layers of isofacial amphibolites occasionally interlayered with fine-grained leucocratic gneisses. The chemical composition indicates a calc-alkaline nature of the precursors (e.g. Wimmenauer 1984; Wimmenauer and Hanel 1997). The igneous detrital zircons and the calc-alkaline nature of the amphibolite intercalations agree with an active margin setting after the Upper Ordovician. Such a setting is proposed for the western part of the future Hun superterrane, particularly for Cadomia, through closure of part of the Rheic ocean and subduction under the northern margin of Gondwana, before the Silurian opening of the Palaeo-Tethys and the final detachment from Gondwana (von Raumer et al. 2002; Stampfli et al. 2002).

The Ordovician detrital subpopulation of the granulite-facies metasediment 91-1c (Unit 3 of the CSGC) has morphological and geochronological features very similar to SB-22. However, in the case of 91-1c, an even younger, but rare detrital component was identified which indicates a younger episode of sedimentation in the Devonian ($< 390 \pm 10$ Ma), followed shortly afterwards by HP-HT granulite-facies metamorphism (335 ± 2 Ma). A Lower to Middle Devonian magmatic episode is so far unknown for the Schwarzwald basement, and also not a generally observed feature of the Moldanubian and Saxothuringian zones of the Variscan fold belt. However, Devonian ages of high-pressure metamorphism, probably related to the collision of Armorica/the western Hun superterrane with Avalonia or fragments thereof, were reported from several klippen in the Saxothuringian (e.g. Münchberg Gneiss Massif; Stosch and Lugmair 1990), from the Massif Central (Pin 1991) and from Galicia (e.g. Marcos et al. 2002). Schäfer et al. (1997) reported detrital zircons and debris of crystalline rocks derived presumably from the Tepla-Barrandian zone with an age of about 380 Ma in Saxothuringian flysch sediments. From single zircon analyses, Anthes and Reischmann (2001) reported Lower Devonian granitoid magmatism for the western part of the Mid-German Crystalline Rise (MGCR, see Fig. 4), originating presumably in response to subduction of the Rhenohercynian ocean from the north. The lowermost zircon ages for the MGCR (398 ± 3 Ma, Zeh et al. 1997; 405 ± 3 Ma, Reischmann et al. 2001) are also within the error of the Devonian age reported in the present study. Another Lower Devonian age of detrital zircons (386 ± 2 Ma), also identical within the error limits, was reported by Schaltegger et al. (1996) from non-metamorphic Famennian sediments from the Southern Vosges volcano-sedimentary basin. The provenance of these zircons is unknown.

All these findings support the suggestion that the sediments of Units 2 and 3 of the CSGC were deposited in marine basins during Siluro (?)/Devonian times.

Implications to zirconology

In the Schwarzwald basement, Carboniferous metamorphism, i.e. low-pressure high-temperature conditions (about 750 °C, 0.42–0.45 GPa) in all units and the preceding granulite-facies conditions (> 950 °C, > 1.5 GPa) in Unit 3 pervasively transformed the precursors of the investigated metasediments to gneisses with metamorphic mineral assemblages. Under these conditions the U-Pb isotopic systems of zircon are expected to be significantly modified, and in certain cases

they are more likely to record the time of metamorphic overprint (e.g. Pidgeon 1992; Vavra et al. 1996; Hoskin and Black (2000). The overall behaviour of the U-Pb system of the detrital zircons from the present study appears different. The intensity of the high-grade metamorphism in the study area was not sufficient to severely obliterate the protolith age information in most of the zircons. A more or less complete set of detrital zircon ages could thus be derived, even in case of peak temperatures approximating 1,000 °C. Various detrital zircon individuals show intense alteration and secondary internal structures due to transgressive recrystallization and element redistribution. However, in many of these cases, the protolith ages are well preserved. The observation of closed-system behaviour of the U-Pb system of zircon under high-grade conditions is in agreement e.g. with the results of Kröner et al. (2000) for high-pressure granulites from Southern Bohemia/Czech Republic. It supports the conclusions of Möller et al. (2002) who reported negligible resetting of Norwegian zircon populations under dry granulite-facies conditions with temperatures >950 °C.

In the investigated samples, only subpopulations with high U and Th contents (several thousand ppm) and a complete breakdown of the zircon lattice by metamictization, followed by subsequent recrystallization in the course of a thermal event, show such a strong readjustment of the U-Pb system that in some cases these U-Pb systems record the subsequent metamorphic event(s). This is relevant for discussions of the geological relevance of zircon age data from high-grade metamorphic zircon. The U-Pb stability of the low U-Th relatively crystalline zircons is in accord with the very low diffusivities of U, Th and Pb (Cherniak et al. 1997; Lee et al. 1997) and the very high closure temperatures for Pb loss in zircon (Lee et al. 1997), indicating that volume diffusion in intact zircon crystals is not the dominant process of Pb loss (Mezger and Krogstad 1997).

In the case of the Schwarzwald samples, the response of detrital zircons to metamorphic overprint and/or the formation of new zircon seems to be more pronounced under granulite-facies, nearly ultra-high-temperature conditions, than in the amphibolite facies. Time estimates e.g. from garnet zoning and the T–t path of HT gneisses and migmatites from the Bayerische Wald suggest a very short thermal peak for the Variscan HT-LP metamorphism (Kalt et al. 2000). This may explain why there is only a minor amount of newly formed zircon in the amphibolite-facies metasediments of Units 1 and 2 and the OGC in the Schwarzwald. The duration of Variscan granulite-facies metamorphism, such as in Unit 3 of the Schwarzwald, could not be estimated. The availability of partial melt may be important. However, greywacke compositions, as represented by the samples of Units 1, 2 and the metasediment from the OGC do not yield much partial melt at temperatures around 750–800 °C (e.g. Stevens et al. 1997). In case of sample 91-1c from CSGC Unit 3, strong influence of partial melts on the genesis of the investigated zircons is not supported by the internal grain morphologies with complete absence of zoning in the Carboniferous zircon phases.

Summary and conclusions

The internal morphologies of many of the investigated detrital zircons from metasediments of the Northern and Central Schwarzwald basement have been considerably modified during different episodes of high-grade metamorphism (up to 1,000 °C). However, in many of the studied individuals, blurring of primary internal morphologies, and generation of secondary structures by recrystallization did not severely obliterate the original age information. This demonstrates that SHRIMP ages derived from detrital zircon populations in high- to ultrahigh-grade metasediments can still reflect the age structure of the sediment provenance.

The investigated metasediments from the OGC and from the three investigated tectonometamorphic units of the CSGC have been deposited during **Palaeozoic** sedimentary cycles. The source rocks of all of the Precambrian detrital zircons have northern Gondwana geochronological signatures, resembling for instance the West African Craton, and related to the marginal belts formed during the Neoproterozoic. No significant sediment influx from Grenvillian provinces (e.g. like those of Amazonia or Baltica) has been observed in the detritus, in contrast e.g. to basement rocks of the Bohemian Massif. On the other hand the studied rocks are similar to the Bohemian rocks in the dominance of Cadomian/pan-African zircons documenting repeated crustal reworking and magmatism in the source rock areas.

Different Palaeozoic evolutions are indicated for the investigated tectonometamorphic units. Metasediments of Units 2 and 3 contain Late Ordovician and Devonian (only Unit 3) detritus. They were presumably located in parts of Gondwana derived microcontinents (e.g. the Hun superterrane sensu Stampfli et al. 2002) that formed their leading edge during accretion to the northern continents. Consolidation of these units took place during diagenesis and metamorphic processes of Carboniferous age. The granulite-facies metamorphism in Unit 3 is precisely dated at 335 ± 2 Ma. Unit 1 and OGC metasediments lack Palaeozoic detritus. They were probably deposited close to a continental environment that later collided with the northern continents in the Viséan and was consolidated for the first time by diagenetic and metamorphic processes in the Early **Palaeozoic** and finally metamorphosed in the Carboniferous.

Acknowledgements We gratefully acknowledge the assistance of A. Wagner and U.A. Glasmacher in preparing the polished mounts, and A. Nemchin and A. Kennedy in running the SHRIMP II in Perth. The SHRIMP II is operated by a consortium consisting of Curtin University of Technology, the University of Western Australia and the Geological Survey of Western Australia, with the support of the Australian Research Council. The project strongly benefited from a grant of the Deutsche Forschungsgemeinschaft

(Ka-1023-6). We greatly appreciate the helpful and constructive reviews of U. Schaltegger and J.F. von Raumer.

References

Aleinikoff JN, Nockleberg WJ (1989) Age of deposition and provenance of the Cleary Sequence of the Fairbanks Schist Unit, Yukon-Tanana Terrane, east-central Alaska. USGS Bull B 1903:75–83

Anthes G, Reischmann Th (2001) Timing of granitoid magmatism in the eastern mid-German crystalline rise. J Geodyn 31:119–143

Bowring SA, Grotzinger JP, Isachsen CE, Knoll AH, Pelechaty SM, Kolosov P (1993) Calibrating rates of Early Cambrian evolution. Science 261:1293–1298

Chen F, Hegner E, Todt W (2000) Zircon ages and Nd isotopic and chemical compositions of orthogneisses from the Black Forest, Germany: evidence for a Cambrian magmatic arc. Int J Earth Sci 88:791–802

Cherniak DJ, Hanchar JM, Watson EB (1997) Diffusion of tetravalent cations in zircon. Contrib Mineral Petrol 127:383–390

Cocks LRM, Torsvik TH (2002) Earth geography from 500 to 400 million years ago: a faunal and palaeomagnetic review. J Geol Soc Lond 159:631–644

Compston W, Williams IS, Meyer C (1984) U-Pb chronology of zircons from lunar breccia 73217 using a sensitive high-resolution ion-microprobe. J Geophys Res 89:525–534

Davis DW, Pezzutto F, Ojakangas RW (1990) The age and provenance of metasedimentary rocks in the Quetico Subprovince, Ontario, from single zircon analyses; implications for Archean sedimentation and tectonics in the Superior Province. Earth Planet Sci Lett 99:195–205

De Laeter JR, Kennedy AK (1998) A double focussing spectrometer for geochronology. Int J Mass Spec 178:43–50

Dörr W, Zulauf G, Fiala J, Franke W, Vejnar Z (2002) Neoproterozoic to Early Cambrian history of an active plate margin in the Teplá-Barrandian unit—a correlation of U-Pb isotopic-dilution-TIMS ages (Bohemia, Czech Republic). Tectonophysics 352:65–85

Eichhorn R, Loth G, Kennedy A (2001) Unravelling the pre-Variscan evolution of the Habach terrane (Tauern Window, Austria) by U-Pb SHRIMP zircon data. Contrib Mineral Petrol 142:147–162

Franke W (2000) The mid-European segment of the Variscides: tectonostratigraphic units, terrane boundaries and plate tectonic evolution. In: Franke W, Haak V, Oncken O, Tanner D (eds) Orogenic processes: quantification and modelling of the Variscan belt. Geol Soc Lond Spec Publ 179:35–61

Friedl G, Finger F, McNaughton NJ, Fletcher IR (2000) Deducing the ancestry of terranes: SHRIMP evidence for South America-derived Gondwana fragments in central Europe. Geology 28:1035–1038

Gebauer D, Williams IS, Compston W, Grünenfelder M (1989) The development of the Central European continental crust since the early Archean based on conventional and ion-microprobe dating of up to 3.84 b.y. old detrital zircons. Tectonophysics 157:81–96

Guerrot C, Peucat JJ (1990) U-Pb geochronology of the Upper Proterozoic Cadomian orogeny in the northern Armoricain Massif, France. In: D'Lemos RS, Strachan RA, Topley CG (eds) The Cadomian Orogeny. Geol Soc Spec Publ 51:13–26

Hanel M, Lippolt HJ, Kober B, Wimmenauer W (1993) Lower Carboniferous granulites in the Schwarzwald basement near Hohengeroldseck (SW-Germany). Naturwissenschaften 80:25–28

Hanel M, Montenari M, Kalt A (1999) Determining sedimentation ages of high-grade metamorphic gneisses by their palynological record: a case study in the northern Schwarzwald (Variscan belt, Germany) Int J Earth Sci 88:49–59

Hanel M, Wimmenauer W (1990) Petrographische Indizien für einen Deckenbau im Kristallin des Schwarzwaldes. Ber Deutsch Min Ges Bh 1 z Eur J Mineral 2:89

Hann HP, Sawatzki G (1998) Deckenbau und Sedimentationasalter im Grundgebirge des Südschwarzwaldes/SW-Deutschland. Z dt geol Ges 149:183–195

Hegner E, Kröner A (2000) Review of Nd isotopic data and xenocrystic and detrital zircon ages from the pre-Variscan basement of the eastern Bohemian massif: speculations on palinspastic reconstructions. In: Franke W, Haak V, Oncken O, Tanner D (eds) Orogenic processes: quantification and modelling of the Variscan belt. Geol Soc Lond Spec Publ 179:113–129

Hofmann A, Köhler H (1973) Whole rock Rb-Sr ages of anatectic gneisses from the Schwarzwald. N Jahrb Miner Abh 119:163–187

Hoskin PWO, Black LP (2000) Metamorphic zircon formation by solid-state recrystallization of protolithic igneous zircon. J Metamorph Geol 18:423–439

Kalt A, Altherr R, Hanel M (2000) The Variscan basement of the Schwarzwald. Ber Deutsch Min Ges Beih z Eur J Mineral 12, 2:1–43

Kalt A, Corfu F, Wijbrans JR (2000) Time calibration of a P–T path from a Variscan high-temperature low-pressure metamorphic complex (Bayerische Wald, Germany), and the detection of inherited monazite. Contrib Miner Petrol 138:143–163

Kalt A, Grauert B, Baumann A (1994) Rb-Sr and U-Pb isotope studies on migmatites from the Schwarzwald (Germany): constraints on isotopic resetting during Variscan high-temperature metamorphism. J Metamorph Geol 12:667–680

Kemnitz H, Romer RL, Oncken O (2002) Gondwana break-up and the northern margin of the Saxothuringian belt (Variscides of Central Europe). Int J Earth Sci 91:246–259

Kober B, Hradetzky H, Lippolt HJ (1986) Radiogenblei-Evaporationsstudien an einzelnen Zirkonkristallen zur prähercynischen Entwicklung des Grundgebirges im Zentralschwarzwald, SW-Deutschland. Fortschr Mineral 64 Bh1:81

Kossmat F (1927) Gliederung des varistischen Gebirgsbaus. Abh Sächs Geol Landesamt 1:1–39

Kröner A, O'Brien PJ, Nemchin AA, Pidgeon RT (2000) Zircon ages for high-pressure granulites from South Bohemia, Czech Republic, and their connection to Carboniferous high-temperature processes. Contrib Mineral Petrol 138:127–142

Lee JWK, Williams IS, Ellis DJ (1997) Pb, U and Th diffusion in natural zircon. Nature 390:159–162

Liew TC, Hofmann AW (1988) Precambrian crustal components, plutonic associations, plate environment of the Hercynian fold belt of central Europe: indications from a Nd and Sr study. Contrib Mineral Petrol 98:129–138

Linnemann U, Gehmlich M, Tichomirova B, Buschmann L, Nasdala P, Jonas H, Lützner H, Bombach K (2000) From Cadomian subduction to early Palaeozoic rifting: the evolution of Saxothuringia at the margin of Gondwana in the light of single zircon geochronology and basin development (Central European Variscides, Germany). In: Franke W, Haak V, Oncken O, Tanner D (eds) Orogenic processes: quantification and modelling of the Variscan belt. Geol Soc Lond Spec Publ 179:131–153

Lippolt HJ, Hradetzky H, Hautmann S (1994) K-Ar dating of amphibole bearing rocks in the Schwarzwald, SW Germany: I. $^{40}Ar/^{39}Ar$ age constraints to Hercynian HT-metamorphism. Neues Jahrb Miner Mh 1994/10:433–448

Lork A, Miller H, Kramm U, Grauert B (1990) U-Pb systematics of detrital zircons from the Puncoviscana Formation and their significance for maximum age of sedimentation in the Sierra de Cachi, Salta, Argentina. Correlation Geologica 4:199–208

Loth G, Eichhorn R, Höll R, Kennedy A, Schauder P, Söllner F (2001) Cambro-Ordovician age of a metagabbro from the Wildschönau ophiolite complex, Greywacke Supergroup (eastern Alps, Austria): A U-Pb SHRIMP study. Eur J Mineral 13:57–66

Ludwig KR (2000) User's manual for Isoplot/Ex version 2.2: a geochronological toolkit for Microsoft Excel. Berkeley Geochronol Center Spec Publ 1a:1–53
Marcos A, Fernandez-Rodriguez FJ, Llana Funez S (2000) Structure of the Cabo Ortegal Nappe. In: Basement tectonics 15, A Coruna:1–59
Marschall H, Kalt A, Hanel M (2003) P–T evolution of a Variscan lower-crustal segment. A study of granulites from the Schwarzwald, Germany. J Petrol 44:227–253
Matte P (2001) The Variscan collage and orogeny (480–290 Ma) and the tectonic definition of Amorica microplate: a review. Terra Nova 13:122–128
McLennan SM, Bock B, Compston W, Hemming SR, McDaniel DK (2001) Detrital zircon geochronology of Taconian and Acadian foreland sedimentary rocks in New England. J Sediment Res 71:305–317
Mezger K, Krogstad EJ (1997) Interpretation of discordant U-Pb ages: an evaluation. J Metamorphic Geol 15:127–140
Möller A, O'Brien PJ, Kennedy A, Kröner A (2002) Polyphase zircon in ultrahigh-temperature granulites (Rogaland, SW Norway): constraints for Pb diffusion in zircon. J Metamorphic Geol 20:727–740
Montenari M (1996) Appearance of microfossils in high-grade metamorphic rocks from SW-Germany. IXth Int Palynol Congr Meeting, Houston, Texas, Abstracts: 110
Montenari M, Servais T, Paris F (2000) Palynological dating (acritarchs and chitinozoans) of lower Palaeozoic phyllites from the Black Forest/southwestern Germany. C R Acad Sci Paris, Earth Planet Sci 330:493–499
Müller H (1989) Geochemistry of metasediments in the Hercynian and pre-Hercynian crust of the Schwarzwald, the Vosges and Northern Switzerland. Tectonophysics 157:97–108
Nance RD, Murphy JB (1996) Basement isotopic signatures and Neoproterozoic paleogeography of Avalonian-Cadomian and related terranes in the circum-North Atlantic. In: Nance RD, Thompson MD (eds) Avalonian and related peri-Gondwanan terranes of the circum-North Atlantic. Geol Soc Am Spec Pap 304:333–346
Nelson DR (2001) An assessment of the determination of depositional ages for Precambrian clastic sedimentary rocks by U-Pb dating of detrital zircons. Sediment Geol 141/142:37–60
Nemchin AA, Pidgeon RT (1997) Evolution of the Darling Range Batholith, Yilgarn Craton, Western Australia: a SHRIMP zircon study. J Petrol 38:625–649
Odin GS (1994) Phanerozoic time scale. Bull Liais Inform USGS Subcom Geochronol 12
Pidgeon RT (1992) Recrystallization of oscillatory zoned zircon: some geochronological and petrological implications. Contrib Miner Petrol 110:463–472
Pidgeon RT, Furfaro D, Kennedy A, Nemchin AA, van Broswjk W (1994) Calibration of zircon standards for the Curtin SHRIMP. USGS Circ 1107:251
Pidgeon RT, Nemchin AA, Hitchen GJ (1998) Internal structures of zircons from Archean granites from the Darling Range batholith: implications for zircon stability and the interpretation of zircon ages. Contrib Miner Petrol 132:288–299
Pin Ch (1991) Central Western Europe: major stages of development during Precambrian and Paleozoic times. In: Dallmeyer RD, Lecorche JP (eds) The West African orogens and circum-Atlantic correlatives, pp 295–306
Rehfeld U (1983) A relictic staurolite-kyanite mineral paragenesis in paragneisses of the Central Schwarzwald. Neues Jahrb Mineral Abh 146:170–181
Reischmann T, Anthes G, Jaeckel P, Altenberger U (2001) Age and origin of the Böllsteiner Odenwald. Mineral Petrol 72:29–44
Robardet M (2003) The Armorica 'microplate': fact or fiction? Critical review of the concept and contradictory palaeobiogeographical data. Palaeogeogr Palaeoclimatol Palaeoecol 195:125–148
Robb LJ, Davis DW, Kamo SL (1990) U-Pb ages on single detrital zircon grains from the Witwatersrand basin, South Africa; constraints on the age of sedimentation and on the evolution of granites adjacent to the basin. J Geol 98:311–328
Rocci G, Bronner G, Deschamps M (1991) Crystalline basement of the West African Craton. In: Dallmeyer RD, Lecorche JP (eds) The West African orogens and circum-Atlantic correlatives. Springer, Berlin Heidelberg New York, pp 31–61
Ross GM, Parrish RR (1991) Detrital zircon geochronology of metasedimentary rocks in the southern Omineca belt, Canadian Cordillera. Can J Earth Sci 28:1254–1270
Rubatto D (2002) Zircon trace element geochemistry: partitioning with garnet and the link between U-Pb ages and metamorphism. Chem Geol 184:123–138
Schäfer J, Neuroth, H, Ahrendt H, Dörr W, Franke W (1997) Accretion and exhumation of a Variscan active margin, recorded in the Saxothuringian flysch. Geol Rundsch 86:599–611
Schaltegger U, Fanning CM, Günther D, Maurin, JC, Schulmann K, Gebauer D (1999) Growth, annealing and recrystallization of zircon and preservation of monazite in high-grade metamorphism: conventional and in-situ U-Pb isotope, cathodoluminescence and microchemical evidence. Contrib Mineral Petrol 134:186–201
Schaltegger U, Gebauer D (1999) Pre-Alpine geochronology of the Central, Western and Southern Alps. Schweiz Mineral Petrogr Mitt 79:79–8
Schaltegger U, Nägler TF, Corfu F, Maggetti M, Galetti G, Stosch HG (1997) A Cambrian island arc in the Silvretta nappe: constraints from geochemistry and geochronology. Schweiz Mineral Petrogr Mitt 77:337–350
Schaltegger U, Schneider JL, Marin JC, Corfu F (1996) Precise U-Pb chronometry of 345–340 Ma old magmatism related to syn-convergence extension in the Southern Vosges (Central Variscan belt). Earth Planet Sci Lett 144:403–419
Scotese CR, McKerrow WS (1990) Revised world maps and introduction. In: McKerrow WS, Scotese CR (eds) Palaeozoic palaeogeography and biogeography. Geol Soc Lond Mem 12:1–21
Söllner F, Nelson DR, Miller H (1997) Provenance deposition and age of gneiss units from the KTB drill hole (Germany): evidence from SHRIMP and conventional U-Pb zircon age determination. Geol Rundsch Suppl 86:235–250
Stampfli GM, Borel GD (2002) A plate tectonic model for the Paleozoic and Mesozoic constrained by dynamic plate boundaries and restored synthetic oceanic isochrons. Earth Planet Sci Lett 196:17–33
Stampfli GM, von Raumer JF, Borel GD (2002) Paleozoic evolution of pre-Variscan terranes: from Gondwana to the Variscan collision. In: Martinez Catalan JR, Hatcher RD, Arenas R, Diaz Garcia F (eds) Variscan-Appalachian dynamics: the building of the late Paleozoic basement. Geol Soc Am Spec Pap 364:263–280
Steiger RH, Bär MT, Büsch W (1973) The zircon age of an anatectic rock in the central Schwarzwald. Fortschr Mineral 50 (Bh 3):131–132
Stevens G, Clemens JD, Droop GTR (1997) Melt production during granulite-facies anatexis: experimental data from 'primitive' metasedimentary protoliths. Contrib Mineral Petrol 128:352–370
Stosch HG, Lugmair GW (1990) Geochemistry and evolution of MORB-type eclogites from the Muenchberg Massif, southern Germany. Earth Planet Sci Lett 99:230–249
Tait JA, Bachtadse V, Franke W, Soffel HC (1997) Geodynamic evolution of the European Variscan fold belt: paleomagnetic and geological constraints. Geol Rundsch 86:585–598
Tait JA, Bachtadse V, Soffel H (1994) Silurian paleogeography of Armorica: new paleomagnetic data from central Bohemia. J Geophys Res 99:2897–2907
Tait JA, Bachtadse V, Soffel H (1995) Upper Ordovician paleogeography of the Bohemian Massif: implications for Amorica. Geophys J Int 122:211–218

Tait JA, Schätz M, Bachtadse V, Soffel H (2000) Paleomagnetism and Paleozoic paleogeography of Gondwana and European terranes. In: Franke W, Haak V, Oncken O, Tanner D (eds) Orogenic processes: quantification and modelling of the Variscan belt. Geol Soc Lond Spec Publ 179:21–34

Tichomirova M, Berger HJ, Koch EA, Belyatski BV, Götze J, Kempe U, Nasdala L, Schaltegger U (2001) Zircon ages of high-grade gneisses in the eastern Erzgebirge (Central European Variscides)—constraints on origin of the rocks and Precambrian to Ordovician magmatic events in the Variscan fold belt. Lithos 56:303–332

Vavra G, Gebauer D, Schmid R, Compston W (1996) Multiple zircon growth and recrystallization during polyphase Late Carboniferous to Triassic metamorphism in granulites of the Ivrea Zone, Southern Alps: an ion microprobe (SHRIMP) study. Contrib Mineral Petrol 122:337–358

von Raumer JF, Stampfli GM, Borel G, Bussy F (2002) Organization of pre-Variscan basement areas at the north-Gondwanan margin. Int J Earth Sci 91:35–52

von Raumer JF, Stampfli GM, Borel G, Bussy F (2003) Gondwana derived microcontinents—the constituents of the Variscan and Alpine collisional orogens. Tectonophysics 365:7–22

Wimmenauer W (1984) Das prävariskische Kristallin im Schwarzwald. Fortschr Mineral 62 Bh 2:69–86

Wimmenauer W, Hanel M (1997) Die Fortsetzung der Randgranit-Assoziation nach Nordosten und Norden. Jh geol Landesamt Baden-Württemberg 37:7–24

Zeh A, Brätz H, Cosca M, Tichomirova M (1997) 39Ar/40Ar und 207Pb/206Pb Datierungen im Ruhlaer Kristallin, Mitteldeutsche Kristallinzone. Terra Nostra 97/5:212–215

Zeh A, Brätz H, Millar IL, Williams IS (2001) A combined zircon SHRIMP and Sm-Nd isotope study of high-grade paragneisses from the Mid-German Crystalline Rise: evidence for northern Gondwanan and Grenvillian provenance. J Geol Soc Lond 158:983–994